Parallel Computational Fluid Dynamics – Advanced Numerical Methods, Software and Applications
B. Chetverushkin, A. Ecer, J. Periaux, N. Satofuka and P. Fox (Editors)

DNS and RANS/LES-computations of complex geometry flows using a parallel multiblock finite-volume code

E. M. Smirnov, A. G. Abramov, N. G. Ivanov, P. E. Smirnov and S. A. Yakubov

Department of Aerodynamics, St.-Petersburg State Polytechnical University,
Polytechnicheskaya 29, St.-Petersburg, 195251, Russia

A parallel version of an in-house 3D multiblock finite-volume code is described. The parallelization of the code is based on the domain decomposition and the introduction of virtual blocks for data exchange at interface regions between neighboring subdomains. Examples of direct numerical simulation and RANS/LES-computations of turbulent flows developing in domains of complex geometry are presented.

1. INTRODUCTION

The parallel capabilities of today's workstation or PC clusters have made possible economical numerical studies of turbulent flows on the base of unsteady formulations in applications to both simplified and complex geometry configurations. Well-known techniques are Direct Numerical Simulation (DNS) and Large Eddy Simulation (LES). However, true or full resolving DNS remains to be extremely time-consuming for Reynolds numbers of more than 10^4. In this situation many authors undertaken attempts for underresolved DNS studies, with surprisingly good results in specific cases. A huge amount of recent contributions was devoted to applications of Large Eddy Simulation (LES) that can be used at much higher Reynolds numbers than DNS. In case of wall-bounded flows, the major difficulties and uncertainties of LES are associated with the treatment of the near-wall layers.

Last years, hybridizations of the Reynolds-averaged Navier-Stokes (RANS) approach with LES become more and more popular. Among various techniques of RANS-LES coupling, the Detached Eddy Simulation (DES) suggested initially for prediction of massively separated turbulent flows [1] is of special interest. The main idea of DES is to entrust the near wall layers to unsteady RANS computations, and the region far away from the wall to LES, using formally the same turbulence model as for the RANS zone, but with a redefined characteristic length responsible for dissipation of turbulence. A comprehensive description of the state-of-the-art in the "standard" DES of massively separated flows is given in [2]. In the standard DES, the boundary layer as a whole is computed with the RANS model, and it is achieved by an appropriate grid generation. In the "non-standard" DES, as applied to internal flow computations [3-4], only a part of the near-wall high-shear layer is treated as the RANS zone. The latter technique may be considered as LES with a specific near-wall treatment avoiding the use of wall functions. Recently promising attempts have been done to perform non-standard DES of the turbulent silicon melt convection in a rotating crucible of a Czochralski

crystal growth system [5] and the strongly turbulent Rayleigh-Benard convection in cubic and cylindrical cells [6].

The present contribution covers recent experience in DNS and RANS/LES-computations of forced and mixed convection turbulent flows with a parallel version of an in-house 3D multiblock finite-volume code being under permanent development since 1992.

2. PARALLEL MULTIBLOCK FINITE-VOLUME CODE

This Section covers peculiarities of parallelization of an in-house 3D steady/unsteady Navier-Stokes code SINF (Supersonic to INcompressible Flows). This code is based on the second-order finite-volume spatial discretization technique using the cell-centered variable arrangement and body-fitted structured (matching or non-matching) grids. The ideas of the artificial compressibility method or the compressibility scaling technique are employed to compute both incompressible and compressible fluid flows. The pseudo-time evolution problem is solved using implicit schemes such as the approximate-factorization scheme or the Gauss-Seidl plane/line relaxation schemes. Dealing with unsteady flows, the pseudo-time iterations are performed for each physical time step. Three-layer second-order scheme was implemented for physical time stepping. Third- and second-order upwind schemes are employed for convective flux evaluation (the QUICK scheme [7] was used for computational examples presented below). For low-speed flows, the solver uses a generalized Rhie-Chow [8] interpolation to avoid de-coupling between velocity and pressure. CUSP-type schemes of Jameson [9] were implemented to handle shock regions of transonic flows. High- and low-Reynolds number versions of several one- and two-parametric differential turbulence models are available for simulation of turbulent flows in the RANS mode. In 2000-2002 the code capabilities were extended to apply the LES and DES techniques.

The parallelization of the code is based on the domain decomposition according to block-structuring of grids, an SPMD (Single Program Multiple Data) strategy, and the MPI standard (Message Passing Interface Forum 1995). The main peculiarities of parallelization concern the data exchange at the interface regions between logical neighboring subdomains. In the non-parallel (prototype) version of the code the boundary updating at the interface of neighboring blocks (after completion of an iteration step) is done via computations within a “virtual” block. This virtual block is formed from near-interface layers of connecting physical blocks, with copying all the data needed for computations of fluxes through the interface. Note that the virtual block concept adopted in the code SINF ensures the conservation of the fluxes at the interface and facilitates solution of many problems associated with the use of non-matching grids and/or with complicated conjugate heat/mass transfer tasks. In the prototype version of the code the virtual block computations are performed sequentially, interface by interface, using the same storage. In order to achieve a high efficiency of parallelization and to avoid the use of a large single master process, copies of near-interface layers of the physical blocks are created in a special process, and the latter performs the interface updating in the same manner as in the serial mode. It is illustrated in Figure 1.

To date, our experience in using the parallel version of the code was limited by using PC clusters of 24 processors or less. For all the flow configurations considered (using grids with size of 0.6 to 2.4 million computational cells), the parallelization efficiency is higher than 0.8.

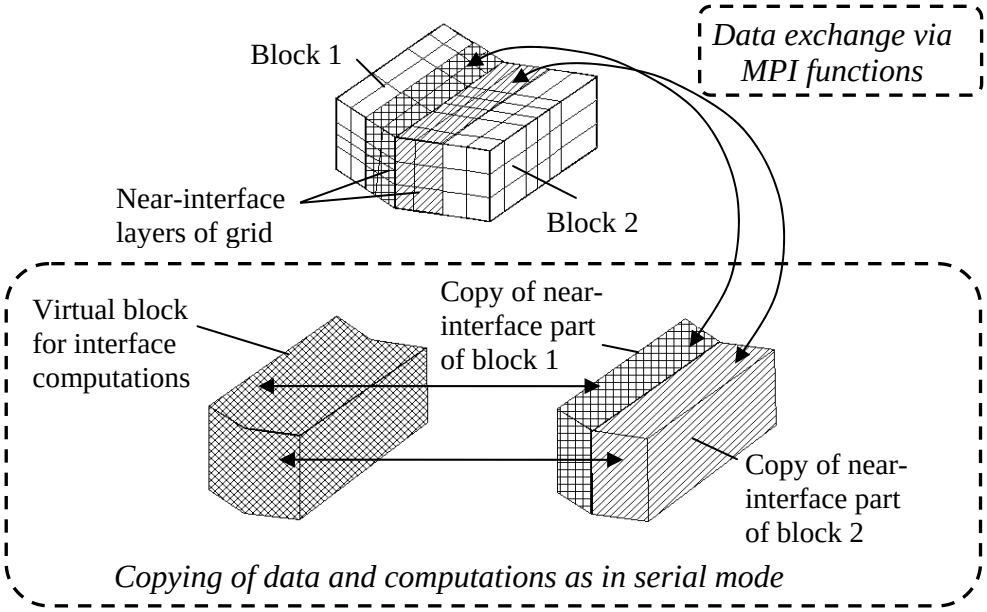

Figure 1. Scheme of data exchange in the parallel version of the code SINF.

3. SOME APPLICATIONS OF THE CODE SINF

3.1. Silicon melt convection in a crucible of a Czochralski crystal growth system

It is well known that low-frequency unsteady 3D oscillations of the molten silicon observed for industrial-scale Czochralski crystal growth systems result in striations of impurity (oxygen) concentration in the crystal and in significant melt temperature fluctuations affecting the crystal defect formation. Typically, velocity fluctuations are comparable or even larger than the local average velocity, and the turbulent transport is mainly controlled by large-scale eddies, the statistical effects of which are very difficult, if possible, to predict on the base of RANS turbulence models. Recently LES and RANS/LES (non-standard DES) were performed for an industrial CZ furnace (EKZ 1300) using a non-parallel version of the code SINF [5, 10]. A computational grid covering the melt convection domain was of about 100,000 cells. With this grid, the thermal unsteady state of the melt and heat transfer features were predicted quite well, as compared with the measurements done for this furnace. However, a qualitative disagreement with experimental data was observed for the oxygen content versus the crucible rotation rate. To discover the reasons of the disagreement, direct numerical simulation of silicon melt turbulent convection at reduced Rayleigh numbers (as compared with the EKZ 1300 prototype) has been performed with the parallel SINF on a grid of next to one million cells.

The domain occupied by Si-melt and boundary conditions used for calculations are shown in Figure 2. With respect to the reference system rotated together with the crucible, the problem is formulated as a non-dimensional one. Note that the dimensional boundary conditions were given in the previous LES computations [10]. The vertical size, H, is taken as the length scale. The doubled temperature difference $\Delta T = 2(T_{max} - T_{melting})$ is assigned to be the temperature scale. The buoyancy velocity, $V_b = (g\beta_T \Delta T H)^{1/2}$, is considered as the velocity scale. The basic geometrical parameters are $R_c/H = 1.7$, $R_s/H = 0.5$. The

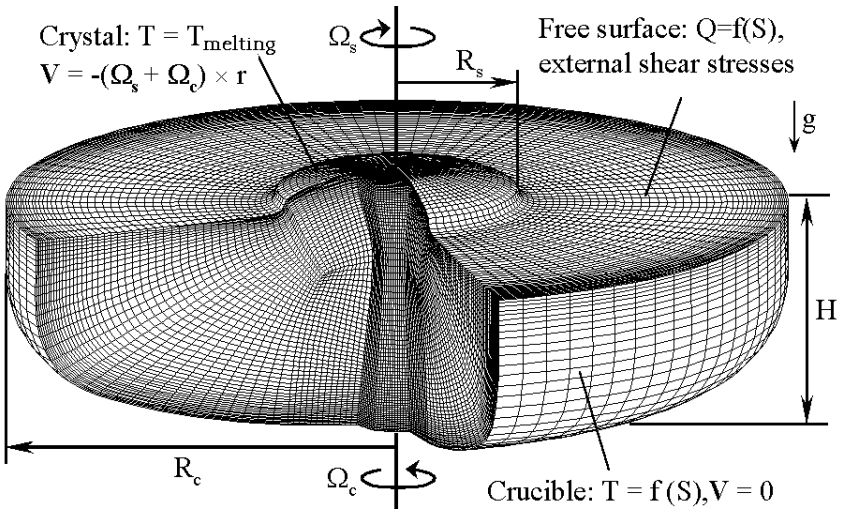

Figure 2. Block-structured computational grid and boundary conditions for direct numerical simulation of turbulent silicon melt convection in a Czochralski crystal growth process.

behaviour of the melt and heat transfer are determined by the Prandtl number, $Pr=\nu/a$, the Rayleigh number, $Ra = g\beta_T(T_{max} - T_{melting})H^3/(\nu a)$, the Rossby number, $Ro = V_b/\Omega_c H$, and the angular velocity ratio, Ω_s/Ω_c.

Figure 3 illustrates instantaneous and time-averaged velocity fields of Si-melt convection at Pr=0.015, $Ra=2.5\times10^6$, Ro=1.9, and $\Omega_s/\Omega_c = -4.0$. One can see that actual velocities are much larger than the averaged those over the major part of the domain, and a very fine resolution is required to get a right statistics near the bottom of the crucible. This conclusion is especially important for the problem of accurate predictions of oxygen transport due to a high value of the Schmidt number that is ranging from 6 to 10. It should be mentioned also that the present DNS

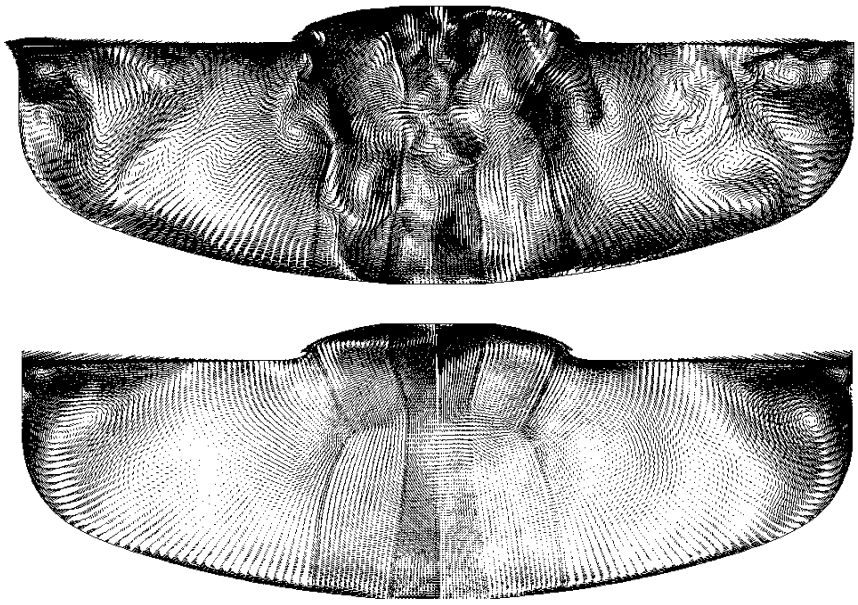

Figure 3. Instantaneous (upper) and time-averaged (lower) velocity fields of silicon melt convection at the Rayleigh number of 2.5×10^6 and the Rossby number of 1.9.

results obtained at a reduced Rayleigh number for (nondimensional) velocity and temperature fields are close to those of RANS/LES obtained with a coarser grid for the real values of Ra. The most remarkably, however, that now the tendency in the oxygen content versus the crucible rotation is closer to the experimental one. Finally, our experience leads to the conclusion that accurate predictions of oxygen transport in industrial-scale CZ furnaces are feasible in the future with RANS/LES computations on grids of about 10 millions cells. No doubt, it is a challenging task for parallel CFD.

3.2. Massively separated flow in a model of a gas turbine exhaust diffuser

This Section concerns predictions of massively separated flows in exhaust diffusers of gas turbines. Typically, a gas turbine exhaust diffuser has inner struts that play several roles in the construction. To minimize pressure losses in the diffuser, profiled strut covers are used in the majority of machines. At off-design conditions, the flow after the gas turbine last stage has a considerable swirl that results in a high incidence and in a massive separation of flow from the profile. When performing numerical simulations of 3D separated flows one usually tries to reduce the problem dealing only with one sector of the diffuser and imposing periodicity boundary conditions in the circumferential direction. It is known, however, that in real unsteady massively separated flows there are pronounced deviations from the circumferential periodicity despite the rotational symmetry of the geometry.

We have performed a study of time-dependent deviations from the circumferential periodicity using an exhaust diffuser model with six real geometry profiled struts (a NACA airfoil). A 360-degrees model of the diffuser shown in Figure 4 was considered. The whole domain was covered by a grid (consisting of six identical sectors) of 2.4 million cells. Direct numerical simulation with no-turbulence model was performed at a Reynolds number of 10^3, based on the bulk inlet velocity and the strut chord. The inlet swirl angle was set to 30 degrees.

Figure 5 presents a snapshot of separated flow past a strut, and a sample illustrating nondimensional streamwise velocity oscillations at compatible monitoring points placed in separation zones of neighboring sectors of the diffuser (solid and dashed curves correspond to different points). One can see that there is a considerable phase shift in leading-frequency oscillations of velocity at compatible monitoring points. However, the statistics of separated

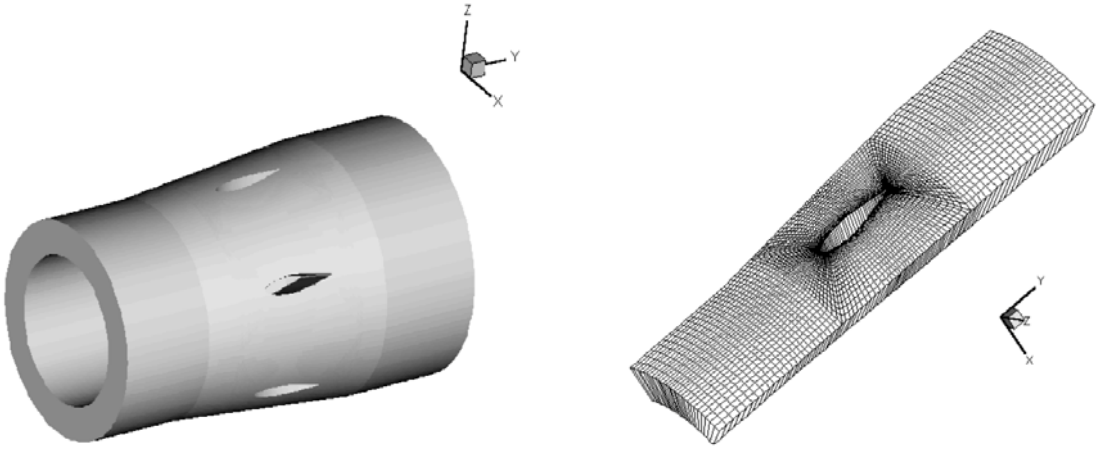

Figure 4. “Solid-gas” model of a gas turbine exhaust diffuser and an H-O-H computational grid for a 60-deg sector of the diffuser.

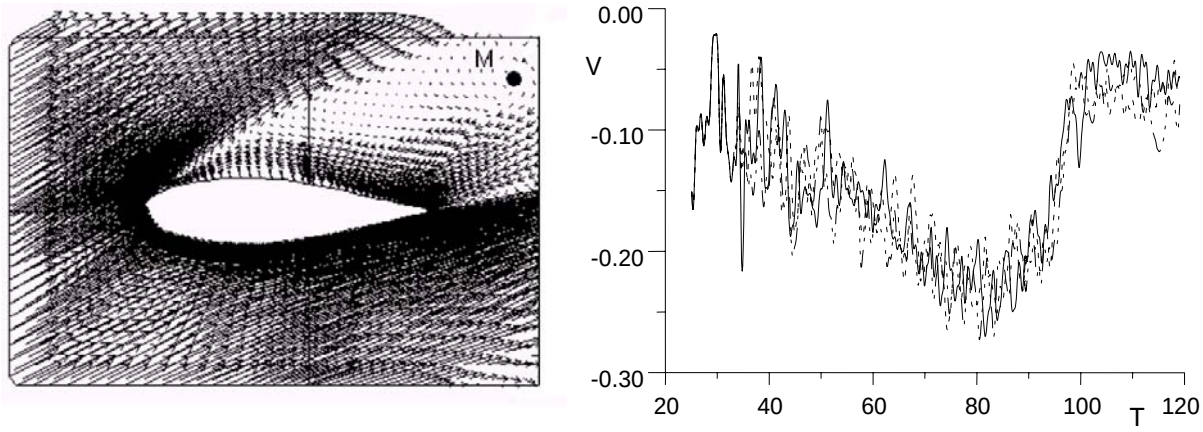

Figure 5. Snapshot of separated flow past a NACA-airfoil strut and velocity oscillations at compatible monitoring points, M, placed in neighboring sectors of the diffuser.

flow in the 360-degrees model is close to that obtained for a 60-degrees model with periodicity boundary conditions imposed. Another interesting observation concerns the development of a "breathing" mode with a characteristic time of about one hundred time units (Figure 5, right).

3.3. Turbulent flow through a single row of square bars

The third computational example is a separated flow through a single row of square bars (Figure 6). In the present work, the row with a pitch three times the bar side is considered (L=3H). The Reynolds number, based on the inlet (uniform) velocity and the bar side, is taken as 10^5, and the case of very low free-stream turbulence is studied. Assuming the bar cascade is unlimited in the pitchwise directions, periodicity conditions should be imposed on corresponding planes of a computational domain. Obviously, the pitchwise size of the computational domain is a free parameter, and it is of certain interest to investigate the influence of this parameter on the flow computed.

First we performed 2D unsteady RANS (URANS) computations using the Spalart-Allmaras turbulence model [11]. The solution domains of one, two and three pitches were

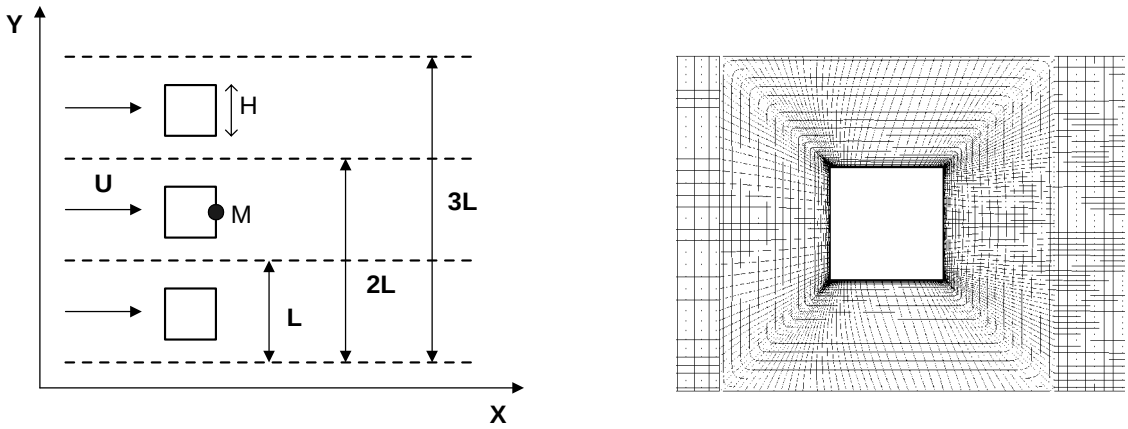

Figure 6. Scheme of flow through a square-bar row and a fragment of an H-O-H grid.

Table 1
Data of 2D URANS and 3D DES computations of flow through a row of square bars

Approach	Domain	Grid, cells	Drag coeff.	RZ-length	Solution
URANS	1 pitch	11,800	3.39	2,47	steady
URANS	1 pitch	14,200	3.48	2,50	steady
URANS	2 pitches	23,600	3.36	0,60	periodic
URANS	2 pitches	28,400	4.38	0,36	periodic
URANS	3 pitches	35,400	3.79	0,84	quasi-periodic
DES	1 pitch	283,200	3.82	2,56	chaotic
DES	2 pitches	566,400	4.02	0,44	chaotic

considered, and the grid sensitivity of the solution was examined (note that only O-parts of the grids were modified in the grid refinement study). It has been established that the pitchwise size of the domain has a dramatic effect on the results of computations. In case of the one-pitch domain, a steady state flow was obtained after a transient process. In case of the two-pitch domain, a periodic flow (illustrated in Figure 7) was computed, and a quasi-periodic flow was obtained for the three-pitch domain. For the time-averaged flow fields, the effect of the domain pitchwise size is mostly pronounced for the length of the recirculation zone (RZ) past a bar (see Table 1). As well, the URANS solutions obtained for the two-pitch and three-pitch domains are very sensitive to a grid refinement.

Then the three-dimensional detached eddy simulation based on the Spalart-Allmaras turbulence model was performed considering a domain of 3H in the spanwise direction. The 3D grids used for DES were obtained by translation of the 2D URANS grids in the spanwise direction. The grids matches the “standard” DES approach activated via substituting for the distance to the nearest wall, d, the new length scale, $\tilde{d} \equiv \min(d, C_{DES}\,\Delta_{DES})$, depending on the local grid spacing, $\Delta_{DES} \equiv \max(\delta_1, \delta_2, \delta_3)$ [1-2].

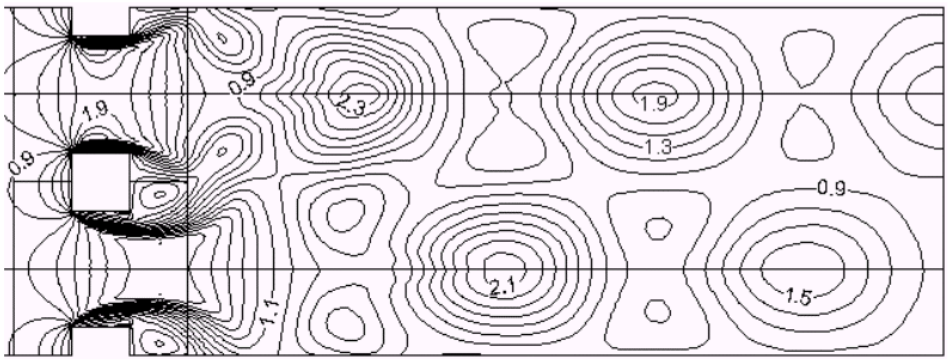

Figure 7. Snapshot of velocity isolines in the two-pitch domain 2D URANS solution.

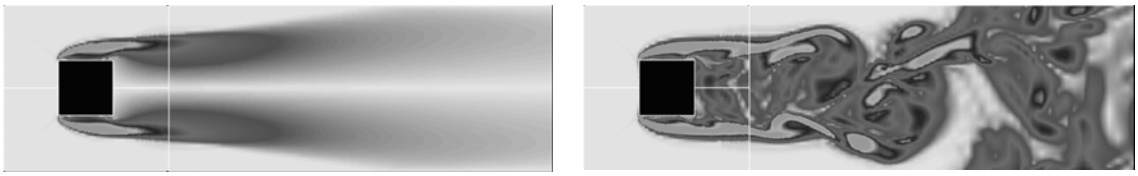

Figure 8. Steady-state vorticity field in the 2D RANS solution (left) and a snapshot of unsteady vorticity field in the 3D DES solution (right) for the one-pitch domain.

In contrast to the 2D RANS approach, the DES produced a time-dependent solution even for the one-pitch domain as illustrated in Figure 8. Remarkably that the pitchwise size of the domain has a dominant effect on DES solutions as well (see Table 1).

ACKNOWLEDGEMENTS

Partially this work was supported by the Russian Foundation for Basic Research under grants No. 01-02-16697 and No. 02-07-90049.

REFERENCES

1. P.R. Spalart, Int J. Heat and Fluid Flow, 21 (2000) 252.
2. M. Strelets, AIAA Paper 2001-0879, (2001).
3. N.V. Nikitin, F. Nicoud, B. Wasistho, K.D. Squires and P.R. Spalart, Phys. Fluids, 12 (2000) 1629.
4. E.M. Smirnov, CD-ROM Proc. of the 12th Int. Heat Transfer Conf., Grenoble, France, (2002).
5. N.G.Ivanov, A.B.Korsakov, E.M.Smirnov, K.V.Khodosevitch, V.V.Kalaev, Yu.N.Makarov, E.Dornberger, J.Virbulis and W.von Ammon, J.Crystal Growth, 250 (2003) 183.
6. A.G. Abramov, N.G. Ivanov and E.M. Smirnov, Proc. of the Eurotherm Seminar 74, Eindhoven, the Netherlands, (2003) 33.
7. B.P. Leonard, Comput. Methods Appl. Mech. Eng., 19 (1979) 59.
8. C.M. Rhie and W.L. Chow, AIAA Journal, 21 (1983) 1525.
9. A. Jameson, Int. J. Num. Meth. Fluids, 20 (1995) 743.
10. I.Yu.Evstratov,V.V.Kalaev,A.I.Zhmakin,Yu.N. Makarov, A.G.Abramov, N.G.Ivanov, E.M.Smirnov, E.Dornberger, J.Virbulis, E.Tomzig and W.von Ammon, J.Crystal Growth, 230 (2001) 22.
11. P.R. Spalart and S.R. Allmaras, La Recherche Aerospatiale, 1 (1994) 5.